2021 43rd Annual International Conference of the
IEEE Engineering in Medicine & Biology Society (EMBC)
Oct 31 - Nov 4, 2021. Virtual Conference

A Comparative Study for Evaluating Passive Shielding of MRI Longitudinal Gradient Coil

Sadeq S Alsharafi*, Ahmed M Badawi* & AbdEl-Monem M El-Sharkawy*

Abstract— **Gradient coils are vital for Magnetic Resonance Imaging (MRI). Their rapid switching generates eddy currents in the surrounding metallic structures of the MRI scanner causing undesirable thermal, acoustic, and field distortion effects. The use of actively shielded gradient coils does not eliminate such undesirable effects totally. Use of passive shielding was proposed lately to particularly help in mitigating eddy currents and loud acoustic noise. Numerical computations are necessary for calculating eddy currents and evaluating the efficacy of passive shielding. Harmonic and temporal eddy current analysis caused by gradient coil(s) using network analysis (NA) can be faster and more flexible than the traditional FDTD and FEM methods. NA was used more than a decade ago but was limited to analyzing eddy currents resulting from z-gradient coils of separated turns. NA with stream function was recently modified resulting in the more general Multilayer Integral Method (MIM) for simulation of eddy currents in thin structures of arbitrary geometries. In this work, we compared the performance of the NA method and an adapted MIM method to analyze eddy current in both the passive shielding and cryostat to the Ansys Maxwell 3D analysis thus evaluating the performance of gradient configurations with and without passive shielding. Both an unconnected and a connected z-gradient coil configuration were used. Our analysis showed high agreement in the profiles of eddy ohmic losses in metallic structures using the three methods. The NA method is the most computationally efficient however, it is limited to specific symmetries unlike the more general MIM and Ansys methods. Our implementation of the adapted MIM method showed computational efficiency relative to Ansys with comparable values. We have developed a computationally efficient eddy current analysis framework that can be used to evaluate more designs for passive shielding using different configurations of MRI gradient coils.**

I. INTRODUCTION

Gradient coils play a significant role in MRI imaging as they encode the MRI signal by creating linearly varying magnetic fields B_z along the different axes (x, y, and z). The longitudinal gradient coil is traditionally responsible for slice selection while the other transverse gradient coils are responsible for spatial encoding of the MRI signal.

The rapid switching of the magnetic field of gradient coils induces eddy currents in surrounding structures such as the cryostat and other neighboring gradient coils. Reducing eddy currents and mitigating their effect is of importance for the performance of MRI where the following techniques can be used; active and passive shielding of gradient coils [1, 2], pre-emphasis of gradient pulses [3], slitting gradient coil tracks [4], using less conductive materials for surrounding structures [5], pulse sequence programming [6], vacuum champers [5] … etc.

Analysis of generated eddy currents is important for gradient coil designs. Several methods have been used to calculate and analyze eddy currents including FDTD, FEM, and NA method [2, 7-10]. Network analysis is generally a fast and effective numerical method where eddy currents are calculated using coupling and resistive mechanism in conducting structures (divided into multi-layer rings) only and do not involve discretization of the whole domain as required in FDTD and FEM. The NA method developed in [2] used the symmetry for the unconnected z-gradient coil to compute eddy currents where the problem was formulated as first-order differential equations or the so-called circuit equations. The studies in [2, 9, 10] used NA to analyze the eddy currents resulting from an unconnected z-gradient coil on the cryostat where the cryostat is discretized into coaxial rings, and the resistances, as well as inductances, were calculated using closed-form equations [2, 9-11]. In that situation, eddy currents were predicted to flow uniformly in circular rings varying along the azimuthal direction where no current was assumed to flow in the longitudinal direction. However, those studies are limited and cannot solve the eddy current problem for connected z-gradient coil or other transverse gradient coils where resulting eddy currents in such cases are not limited to a circular path. Also, there is another limitation for computing eddy currents in non-homogeneous metallic structures.

The MIM [12] is a more general approach that is also based on network analysis and stream functions. The cryostat is divided into multi-layers of meshed triangular elements. The current density is assumed to be uniform in the cross-section of each triangle element, and no current flows between the different layers. The eddy current problem is also represented by a first-order equation to solve stream function values [13, 14] at the nodes of the triangular elements. The source coil could be assumed as a thin-wire or a wire with finite track width.

In this paper, we develop an efficient computational framework for MRI eddy current analysis using both the NA and adapted MIM methods. We compare computational values of eddy currents and efficiencies against a reference FEM method while evaluating the efficacy for two passive shielding configurations (capped and uncapped) involving a longitudinal MRI gradient coil. With careful implementation, this comparative study shows that the three methods can achieve comparable values for eddy ohmic losses albeit at different computational speeds and modeling limitations.

Sadeq S. Alsharafi is financially supported for his Ph.D program at Cairo University by the Yemeni ministry of higher education.
*Sadeq S Alsharafi, Systems and Biomedical Engineering, Cairo University, Giza, Egypt. (e-mail: s.alsharafi@eng-st.cu.edu.eg)
*Ahmed M Badawi, Systems and Biomedical Engineering, Cairo University Giza, Egypt. (e-mail: ambadawi@eng1.cu.edu.eg)
*AbdEl-Monem M El-Sharkawy,Systems and Biomedical Engineering Cairo University, Giza, Egypt (e-mail: abdshark@eng1.cu.edu.eg)

II. Methods And Numerical Simulations

A. Network Analysis (NA)

For axisymmetric problems such as z-gradient and cylindrical metallic structures, the conductors such as cryostat and passive shield are sliced into n concentric rings of finite width w and thickness t smaller than the skin depth (δ) which can be calculated as given:

$$\delta = \sqrt{\frac{1}{\pi \mu f}} \tag{1}$$

Where μ is the permeability of the conductor and f is the frequency of the excitation current. The resistance, self-inductance, and mutual inductance between the rings are calculated as suggested in [2, 9-11] and they are used to calculate the eddy current $\boldsymbol{i}$ in the following circuit equation:

$$\boldsymbol{M}\frac{d\boldsymbol{i}}{dt} + \boldsymbol{R}\,\boldsymbol{i} = -\boldsymbol{M_0}\frac{ds(t)}{dt} \tag{2}$$

$$\boldsymbol{M} = \begin{bmatrix} L_1 & M_{12} & M_{13} & \blacksquare & M_{1n} \\ M_{21} & L_2 & M_{23} & \blacksquare & M_{2n} \\ M_{31} & M_{32} & L_3 & \blacksquare & M_{3n} \\ \blacksquare & \blacksquare & \blacksquare & \blacksquare & \blacksquare \\ M_{n1} & M_{n1} & M_{n1} & \blacksquare & L_n \end{bmatrix}$$

$$\boldsymbol{R} = \begin{bmatrix} R_1 & 0 & 0 & \blacksquare & 0 \\ 0 & R_2 & 0 & \blacksquare & 0 \\ 0 & 0 & R_3 & \blacksquare & 0 \\ \blacksquare & \blacksquare & \blacksquare & \blacksquare & \blacksquare \\ 0 & 0 & 0 & \blacksquare & R_n \end{bmatrix}$$

$$\boldsymbol{i} = \begin{bmatrix} i_1 \\ i_2 \\ i_3 \\ \vdots \\ i_n \end{bmatrix} \qquad \boldsymbol{M_0} = \begin{bmatrix} M_{01} \\ M_{02} \\ M_{03} \\ \vdots \\ M_{0n} \end{bmatrix}$$

Where $\boldsymbol{M}$ is the inductance matrix containing the self-inductances of the rings and the mutual inductances between the rings, $\boldsymbol{R}$ is the resistance matrix contains the resistance of the rings, n is the number of the rings, $\boldsymbol{M_0}$ is the mutual inductance between the rings and the source coil, and $s(t)$ is the current source. A single frequency of sinusoidal current is used in harmonics eddy current analysis while a pulse of a trapezoidal form is used for transient analysis.

For harmonic analysis, the eddy currents vector is given as:

$$\boldsymbol{i} = -j\,\omega\, i_0\,(j\,\omega\,\boldsymbol{M} + \boldsymbol{R})^{-1}\,\boldsymbol{M_0}$$

Where i_0 is the amplitude of the sinusoidal current source, ω is the angular frequency ($2\pi f$), and j is the imaginary unit. For simplicity, the impedance matrix $\boldsymbol{Z}$ can be written as:

$$\boldsymbol{Z} = j\,\omega\,\boldsymbol{M} + \boldsymbol{R} \tag{3}$$

And the harmonic eddy current solution is:

$$\boldsymbol{i} = -j\,\omega\, i_0\,\boldsymbol{Z}^{-1}\,\boldsymbol{M_0} \tag{4}$$

B. Multilayer Integral Method (MIM)

In this method, the metal structures are divided into multiple layers with thickness less than the skin depth (δ) and the surface of each layer is meshed into triangular elements. Each triangle node is locally numbered clockwise or counterclockwise from 1 to 3 [13, 14].

The current density $\vec{J}$ flowing through the surface are represented by stream function Φ as:

$$\vec{J} = \nabla\, x(\Phi.\hat{n}) \tag{5}$$

Where $\hat{n}$ is the normal vector to the surface. The current $\overrightarrow{J_e}$ that flows inside a triangle element depends on the stream function values at the nodes and can be given as:

$$\overrightarrow{J_e} = \overrightarrow{e_1}\,\phi_1 + \overrightarrow{e_2}\,\phi_2 + \overrightarrow{e_3}\phi_3 \tag{6}$$

Where $\overrightarrow{e_1}, \overrightarrow{e_2}, \overrightarrow{e_3}$ the vector facing the triangle nodes (1, 2, and 3) divided by the double area of the triangle, and ϕ_1, ϕ_2, ϕ_3 are the stream function values at the triangle nodes.

The source coil can be considered as a thin wire coil, carrying a time-varying current $s(t)$. The coil is discretized into L segments and the vector of each segment l_k is given as:

$$\overrightarrow{l_k} = l_x\,\hat{x} + l_y\,\hat{y} + l_z\,\hat{z} \tag{7}$$

Where l_x, l_y, and l_z are the segment vector components in the directions of x, y, and z respectively.

The circuit equation is derived from the total electromagnetic energy [12, 13] and can be expressed in the frequency domain as:

$$(\boldsymbol{R_{nm}} + j\omega\boldsymbol{M_{nm}})\boldsymbol{\Phi} = -j\omega\, i_0\,\boldsymbol{M_{n0}} \tag{8}$$

Where $\boldsymbol{\Phi}$ is a vector containing the stream function values of all nodes of conducting structures, $\boldsymbol{M_{n0}}$ is a vector containing the mutual inductance between the nodes n of the meshed metallic structures and the segments of the source coil, $\boldsymbol{R_{nm}}$ is the resistance matrix and $\boldsymbol{M_{nm}}$ is the inductance matrix due to the interaction of any arbitrary nodes n and m, ω is the angular frequency and i_0 is the amplitude of the sinusoidal current passing through the coil. The impedance matrix $\boldsymbol{Z_{nm}}$ can be written as:

$$\boldsymbol{Z_{nm}} = \boldsymbol{R_{nm}} + j\omega\boldsymbol{M_{nm}} \tag{9}$$

The harmonic solution of stream function can be expressed similar to equation (4) as:

$$\boldsymbol{\Phi} = -j\omega\, i_0\,\boldsymbol{Z_{nm}^{-1}}\,\boldsymbol{M_{n0}} \tag{10}$$

Assuming the surface is meshed into a single layer, the nodes n and m are shared among triangles N and M respectively, thus the resistance (R_{nm}) and inductance (M_{nm}) elements can be expressed as:

$$R_{nm} = \frac{1}{\sigma t}\sum_N \sum_M \int_s \vec{e}_{nN}\,.\,\vec{e}_{mM}\;ds \tag{11}$$

$$M_{nm} = \frac{\mu_0}{4\pi}\sum_N \sum_M \int_{s'} \int_s \frac{\vec{e}_{nN}\,.\,\vec{e}_{mM}}{|r_M - r_N|}\,ds\,ds' \tag{12}$$

Where μ_0 is the vacuum permeability which equals $4\pi \times 10^{-7}\,\mathrm{H.m^{-1}}$, σ is the conductivity of the material, t is the thickness of the triangle, $\vec{e}_{nN}$ is the vector facing the node n (which is part of the triangles N) divided by the triangle's area, $\vec{e}_{mM}$ is the vector facing the node m (which is part of the triangles M) divided by the triangle's area, ds and ds' are the surface area element of the triangles in N and M respectively. Notice that equation (11) is valid only for the nodes n and m that share the same triangle(s), otherwise R_{nm}= 0. $|r_N - r_M|$ is the distance between the triangles in N and M. Simply, the distance could be the central difference between the two centroids of the triangles in N and M; however, for better accuracy and to avoid singularities as well as not to reduce computational efficiency we used a 3-points distance calculation.

The mutual inductance elements M_{n0} between the coil's segments and the node n on the metallic structures are calculated as follows:

$$M_{n0} = \frac{\mu_0}{4\pi} \sum_{k=1}^{L} \sum_{N} \int_{s} \frac{\vec{l}_{\mathrm{k}} \cdot \vec{\mathrm{e}}_{nN}}{|r_N - r_k|} \, ds \tag{13}$$

Where $\vec{l}_k$ is the vector of the coil segment k, L is the number of segments on the coil, $|r_N - r_k|$ is the distance between the center of the coil segments and the triangles N who share node n. To ensure no current crosses the boundaries of metallic structures, the stream function at the boundary nodes of each metallic structure should be equal to the same value which is unknown and needs to be determined. For each separate boundary, a different stream function value should be considered (it can take a value of zero at one of the boundaries). The circuit equations are thus modified accordingly to satisfy the boundary conditions where the dimension of the vector $\mathbf{\Phi}$ is reduced to only contain independent stream function variables using a transformation matrix as suggested in [13].

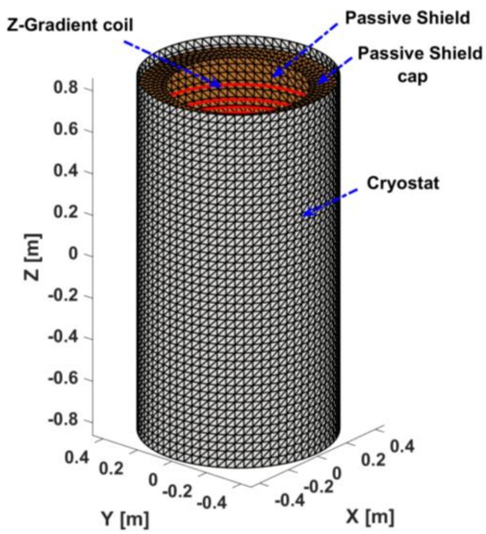

Fig.1: A 3D plot for the complete model including the self-shielded z-gradient coil and the metallic structures (the capped passive shield and scanner's cryostat) which are meshed into triangular elements for MIM.

C. The simulations

The same dimension of the actively shielded z-gradient coil used in [1] is modeled here as a thin wire and is used to induce eddy currents on the cryostat. The same capped and uncapped passive shielding dimensions as [1, 2] were also used. The coil's driving current is assumed to be 100A at a frequency of 1kHz. The z-gradient coil had a primary coil radius of 330mm and a secondary coil radius of 420 mm. Fig.1 shows a 3D plot of the cryostat with the capped-passive shield including the z-gradient coil. The cryostat is a cylinder with a diameter of 903 mm, a height of 1700 mm, and has a thickness of 3.18 mm (less than the skin depth at 1KHz). The cryostat material is stainless-steel with a resistivity of $96\, x\, 10^{-8}\, \Omega$.m. The passive shield is a copper cylinder of 884mm diameter, 1600mm height, and thickness of 1mm (less than the skin depth at 1KHz). The cap of the passive shield has a hole with radius 322 mm and a thickness of 1 mm. The resistivity used for copper is $1.7\, x\, 10^{-8}\, \Omega$ m.

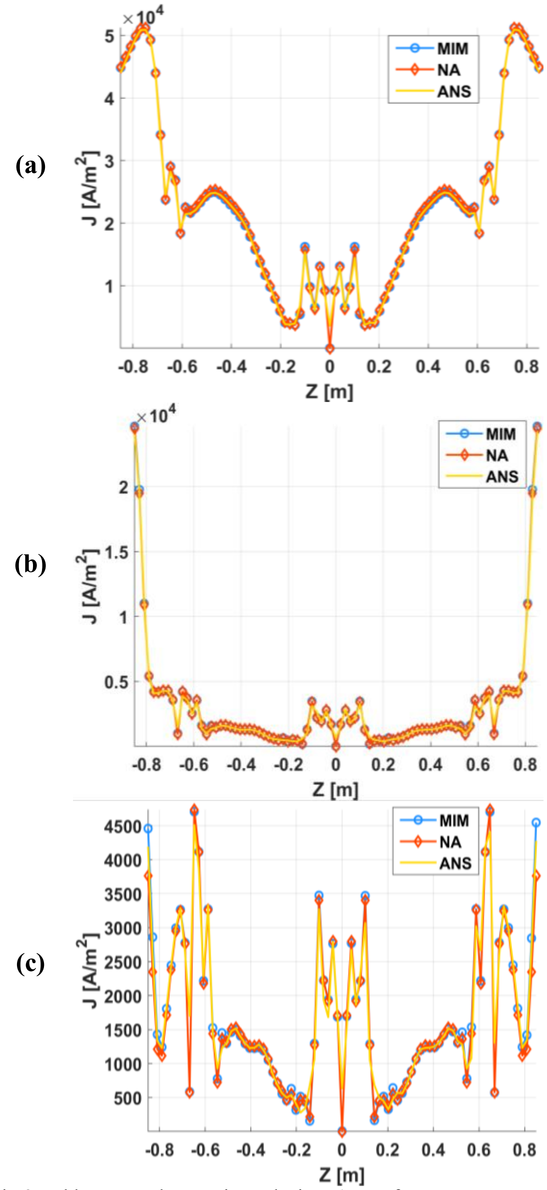

Fig.2: Eddy current harmonic analysis at 1KHz for an unconnected z-gradient coil (circular symmetry is assumed) using the three computational methods. The graph represents the eddy current density profile along the z-direction in the cryostat for the case of: (a) no passive-shielding. (b) non-capped solid passive-shield. (c) capped solid passive-shield.

We implemented the network analysis method [2] and adapted the MIM method [12] using Matlab (MathWorks, MA). In the network analysis computations, the cryostat, passive shield, and cap are sliced into rings with width of 20 mm. For the adapted MIM computations, the metallic structures, including cryostat and passive-shield were meshed into structured triangular elements with a maximum edge length of 20 mm. We also implemented the meshing using Matlab. The driving coils of the z-gradient were segmented with a maximum segment length of 20 mm. To increase the speed of the simulations, nested loops were avoided as much as possible using operations vectorization. To validate our results, the same coil and metallic structures were modeled using Ansys Maxwell 3D (Ansys, Inc., PA). All computations were performed on an Intel (R) Core(TM) i7 (6th generation) CPU (2.60 GHz) laptop with 16 GB RAM.

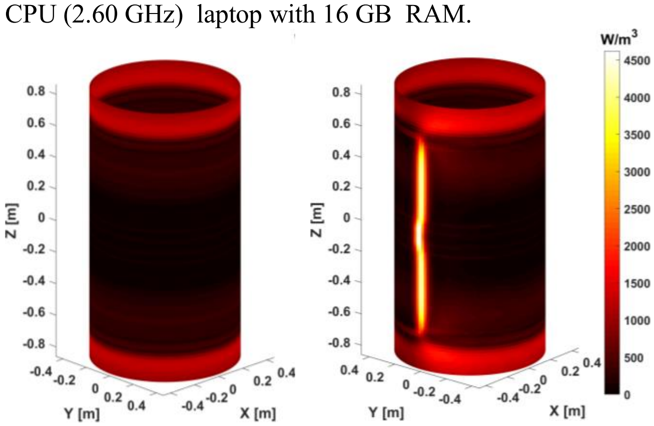

Fig.3: A 3D plot of eddy current ohmic losses for the unconnected (left) and connected z-gradient coils (right) with no passive shielding using the adapted MIM computations. Circular symmetry for the computations is apparent for the unconnected gradient coil.

Table I: TOTAL POWER DISSIPATION (PD) IN THE CRYOSTAT AND THE SIMULATION TIME.

Z-gradient	Passive-Shield	NA (PD/Time)	MIM (PD/Time)	ANS (PD/Time)
Separated	Absent	37.31dBm/ 0.43s	37.28dBm/ 8.04min	37.23dBm/ 4.5h
Connected	Absent	*	38.32dBm/ 8.04min	38.76dBm/ 6h
Separated	Uncapped	23.60dBm/ 1.33s	23.67dBm/ 41.16min	23.51dBm/ 5.1h
Connected	Uncapped	*	23.91dBm/ 43.98min	23.76dBm/ 6.85h
Separated	Capped	14.69dBm/ 1.52s	14.97dBm/ 51.54min	15.00dBm/ 5.75h
Connected	Capped	*	16.52dBm/ 53.34min	16.53dBm/ 6.9h

*The Eddy current cannot be calculated by NA method due lack of circular symmetry.

III. RESULTS AND DISCUSSION

The eddy current density A/m^2, ohmic loss W/m^3, and total power dissipation in dBm were calculated in the cryostat and the passive shield. In case of no passive shielding, Fig.2 shows a comparison of the eddy current density profiles induced by an unconnected, actively shielded z-gradient coil in the cryostat along the z-direction using the three computational methods for the unshielded cases (a), uncapped passive shielding (b) and capped passive shielding (c).

Both the unconnected and connected, actively shielded, z-gradient coil models were simulated at 1KHz using the adapted MIM method. Fig.3 shows the resultant eddy current ohmic losses in the cryostat demonstrating the lack of circular symmetry for the connected model. Lack of symmetry for the more realistic, connected z-gradient model makes the simulation using the NA method [2, 9, 10] inapplicable thus eddy current power losses are only calculated using the adapted MIM method and Ansys in this case. Table I shows a comparison of three techniques in terms of the calculated eddy power losses in the cryostat and the speed of computations for the various configurations that were computed.

IV. CONCLUSION

The computed eddy current results using both the NA and adapted MIM methods for the modeled configurations closely agreed with Ansys computations albeit at a higher computational efficiency. As previously stated, our results confirm that the NA method is highly computational efficient, however, it can only be applied to certain configurations of circular symmetries. We adapted here the MIM method as a more general solution while achieving good computational efficiency. We employed here efficient meshing as well as 3-points distance calculations for calculating the elements of the inductance matrix to achieve acceptable accuracies as well as to reduce the computational load. To increase the speed of the simulations, nested loops were avoided as much as possible using operations vectorization. Our efficient computational framework will allow us to perform both harmonic and transient eddy current analysis for more complex/realistic gradient configurations/situations including transverse gradients where we can evaluate other passive shielding designs as well.

REFERENCES

[1] W. A. Edelstein *et al.*, "Active-passive gradient shielding for MRI acoustic noise reduction," *Magnetic Resonance in Medicine,* vol. 53, no. 5, pp. 1013-1017, 2005.

[2] T. K. Kidane *et al.*, "Active-passive shielding for MRI acoustic noise reduction: Network analysis," *IEEE transactions on magnetics,* vol. 42, no. 12, pp. 3854-3860, 2006.

[3] C. Ahn and Z. Cho, "Analysis of the eddy-current induced artifacts and the temporal compensation in nuclear magnetic resonance imaging," *IEEE transactions on medical imaging,* vol. 10, no. 1, pp. 47-52, 1991.

[4] F. Tang, F. Freschi, M. Repetto, Y. Li, F. Liu, and S. Crozier, "Mitigation of Intra-coil Eddy Currents in Split Gradient Coils in a Hybrid MRI-LINAC System," *IEEE Transactions on Biomedical Engineering,* vol. 64, no. 3, pp. 725-732, 2016.

[5] W. A. Edelstein, R. A. Hedeen, R. P. Mallozzi, S.-A. El-Hamamsy, R. A. Ackermann, and T. J. Havens, "Making MRI quieter," *Magnetic Resonance Imaging,* vol. 20, no. 2, pp. 155-163, 2002.

[6] F. Hennel, F. Girard, and T. Loenneker, "“Silent” MRI with soft gradient pulses," *Magnetic Resonance in Medicine,* vol. 42, no. 1, pp. 6-10, 1999.

[7] X. Li, L. Xia, W. Chen, F. Liu, S. Crozier, and D. Xie, "Finite element analysis of gradient z-coil induced eddy currents in a permanent MRI magnet," *Journal of Magnetic Resonance,* vol. 208, no. 1, pp. 148-155, 2011.

[8] F. Liu and S. Crozier, "An FDTD model for calculation of gradient-induced eddy currents in MRI system," *IEEE transactions on applied superconductivity,* vol. 14, no. 3, pp. 1983-1989, 2004.

[9] M. Sablik, R. Beissner, and A. Choy, "An alternative numerical approach for computing eddy currents: Case of the double-layered plate," *IEEE transactions on magnetics,* vol. 20, no. 3, pp. 500-506, 1984.

[10] T. Takahashi, "Numerical analysis of eddy current problems involving z gradient coils in superconducting MRI magnets," *IEEE transactions on magnetics,* vol. 26, no. 2, pp. 893-896, 1990.

[11] F. W. Grover, *Inductance calculations: working formulas and tables*. Courier Corporation, 2004.

[12] H. Sanchez Lopez *et al.*, "Multilayer integral method for simulation of eddy currents in thin volumes of arbitrary geometry produced by MRI gradient coils," *Magnetic resonance in medicine,* vol. 71, no. 5, pp. 1912-1922, 2014.

[13] A. Kameari, "Transient eddy current analysis on thin conductors with arbitrary connections and shapes," *Journal of Computational physics,* vol. 42, no. 1, pp. 124-140, 1981.

[14] R. A. Lemdiasov and R. Ludwig, "A stream function method for gradient coil design," *Concepts in Magnetic Resonance Part B: Magnetic Resonance Engineering: An Educational Journal,* vol. 26, no. 1, pp. 67-80, 2005.